A review of the dynamic modelling technique of human articulating joints as proposed by Moeinzadeh

A Review of the Dynamic Modelling

Technique of Human Articulating

Joints as Proposed by Moeinzadeh

C.W. Rademaker

Report nr.: WFW 94.038

A Review of the Dynamic Modelling Technique of Human Articulating Joints as Proposed by Moeinzadeh

WFW Report nr: 94.038

Author: Ir. C.W. Rademaker

Supervisors: Prof. dr. ir. J.S.H.M. Wismans (TUE/TNO-WT)
Dr. ir. J.G.M. Thunnissen (TNO-WT)

Eindhoven, July 1994

Computational and Experimental Mechanics Group
Department of Mechanical Engineering
Eindhoven University of Technology (TUE)

Contents

1. Introduction

Injuries resulting from motor vehicle crashes are one of the leading causes of death and disability in modern society. Due to increased safety measures concerning vehicle occupant protection, imposed on motor vehicles by the authorities, it has become essential for the automotive industry to already encorporate possible safety aspects in the earliest design stages.

A prerequisite to establish the effectiveness of these protective safety measures in motor vehicles, such as seat belts and airbags, is the introduction and improvement of crash dummies and mathematical models of human beings. In order to approximate the human behaviour as closely as possible, modifications are done with the aid of experimental results.

The most sophisticated versions of the total-human-body models are articulated and multi-segmented to simulate all the major articulating joints and segments of the human body. Effectiveness of the multisegmented models to accurately predict live human response depends heavily on the proper biomechanical description and simulation of the articulating joints.

The body segments of human beings are usually modelled as rigid bodies. The joints, which connect the body segments and enable relative motion, are often modelled as ball and socket joints or revolute joints. These joints enable relative rotations. These joints suffice for the description of normal motion of human beings but are not applicable in the case of crash simulations in which large rotations and translations take place in a short time interval.

This report has been written within the scope of a project supervised by the TNO Road Vehicles Institute. The aim is to formulate and implement a human joint model which is capable of describing anatomically correct joint motion. The technique needs to be implemented in MADYMO. MADYMO is a combined finite element/multibody program which is used to determine vehicle-occupant interaction. It is developed by the TNO Crash Safety Research Centre in Delft, the Netherlands.

The primary step in obtaining a formulation of human articulating joints is a review of the available literature concerning anatomical joint modelling techniques. Several anatomical joint modelling techniques have been described in the literature. However, these techniques have mainly been applied to the description of the characteristics of the human knee during passive or quasi-static motion. In general, not much has been published in literature concerning the dynamic modelling of human articulating joints. In fact, Hefzy and Grood (1988) concluded that there were only two available dynamic models of the human knee namely those proposed by Moeinzadeh et al. (1983) and Wongchaisuwat (1984).

In this report, a formulation to describe 3-dimensional dynamic human joint motion is reviewed. The formulation was initially developed by Moeinzadeh (1981), and improved and expanded in subsequent papers. In Chapter 2, a human articulating joint is defined by contact surfaces of 2 body segments which execute a relative dynamic motion within the constraints of ligament forces. The generalized description proposed by Moeinzadeh is modified for new purposes and a uniform nomenclature is introduced. In Chapter 3, several numerical procedures are discussed to solve the resulting system of nonlinear differential equations of motion and algebraic contact conditions and geometric compatibility condition. In Chapter 4, the focus is on the specific application of the technique to a 2-dimensional model of the human knee joint: the joint between the femur and tibia. The technique is implemented in MADYMO and the knee model is used for validation. In Chapter 5, several possible improvements of the modelling technique are discussed.

2. Mathematical Formulation of an Articulating Joint

2.1 Introduction

Most mathematical joint models that consider both the geometry of the joint surfaces and behaviour of the joint ligaments are quasi-static in nature and employ the inverse method (Wismans, 1980 & Blankevoort, 1991). The inverse method implies that the ligament forces caused by a specified set of translations and rotations along the specified directions are determined by comparing the geometries of the initial and displaced configurations of the joint. It is furthermore necessary to specify the external force required for the preferred equilibrium configuration. Such an approach is only applicable in a quasi-static analysis. In a dynamic analysis, the equilibrium configuration of the joint is not known and a mathematical analysis is required to provide the equilibrium configuration.

The mathematical description of an articulating joint, which will be described in this chapter, was initially defined by Moeinzadeh (1981). An articulating joint is hereby modelled by two body segments connected by nonlinear springs simulating the ligaments. As deformability of the surfaces of the segments is not taken into account, the body segments are considered to be rigid. Moeinzadeh assumes that one body segment is rigidly fixed, although this assumption has no specific physical applications and is not a condition for describing relative motion between body segments, while the second body segment is able to undergo a three-dimensional dynamic motion (translation and rotation) relative to the fixed body segment. The friction force between the articulating surfaces will be neglected because the coefficients of friction between the articulating joints are assumed to be negligible. This assumption is valid due to the presence of synovial fluid between the articulating surfaces.

2.2 Characterization of the Relative Positions

The position of the moving body segment 1 relative to fixed body segment 0 is described by two coordinate systems as shown in Figure 1. The inertial coordinate system (x^0,y^0,z^0) with unit vectors $\vec{e}_1^{\,0}$, $\vec{e}_2^{\,0}$ and $\vec{e}_3^{\,0}$ is connected to the fixed body segment and the coordinate system (x^1,y^1,z^1) with unit vectors $\vec{e}_1^{\,1}$, $\vec{e}_2^{\,1}$ and $\vec{e}_3^{\,1}$ is attached to the center of mass of the moving body segment. In this report, the following convention is adopted for vector quantities: unit vectors are designated as $\vec{e}$ (superscripts 0 and 1 denote fixed body and moving body segments coordinate systems respectively and integer subscripts denote principal axes) and position vectors by $\vec{r}$ (here a subscript denotes a point on a body segment). The nomenclature has been slightly modified from the original references to give more insight into the mathematical description.

The motion of the moving system (x^1,y^1,z^1) relative to the fixed system (x^0,y^0,z^0) may be characterized by 6 quantities: the translational movement of the origin of the moving system relative to the fixed system in the x,y and z directions, and possible rotations about the x, y and z axes. Let the position vector $\vec{r}_M^{\,0}$ of the origin of the moving body segment coordinate system relative to the fixed body segment coordinate system be given by:

$$\vec{r}_M^{\,0} = x_M^0\,\vec{e}_1^{\,0} + y_M^0\,\vec{e}_2^{\,0} + z_M^0\,\vec{e}_3^{\,0} \qquad (1)$$

Let the vector $\vec{r}_Q^{\,1}$ be the position of an arbitrary point Q on the moving body segment in the base $(\vec{e}_1^{\,1},\vec{e}_2^{\,1},\vec{e}_3^{\,1})$ and let $\vec{r}_Q^{\,0}$ be the position vector of the same point in the base $(\vec{e}^{\,0}_1,\vec{e}^{\,0}_2,\vec{e}^{\,0}_3)$. This can be formulated in the following equations:

$$\vec{r}_Q^{\,1} = x_Q^1\,\vec{e}_1^{\,1} + y_Q^1\,\vec{e}_2^{\,1} + z_Q^1\,\vec{e}_3^{\,1} \tag{2}$$

$$\vec{r}_Q^{\,0} = x_Q^0\,\vec{e}_1^{\,0} + y_Q^0\,\vec{e}_2^{\,0} + z_Q^0\,\vec{e}_3^{\,0} \tag{3}$$

The vectors $\vec{r}_Q^{\,1}$ and $\vec{r}_Q^{\,0}$ have the following relationship (Figure 1):

$$\underline{r}_Q^0 = \underline{r}_M^0 + [\,\underline{T}\,]^T \underline{r}_Q^1 \tag{4}$$

where $\underline{r}$ represents the column definition of the vector notation and $[\,\underline{T}\,]$ is a 3x3 orthogonal transformation matrix which transforms the base of the moving body segment in the base of the fixed body segment. The angular orientation of the (x^1,y^1,z^1) system with respect to the (x^0,y^0,z^0) system is specified by the 9 components of the transformation matrix and is determined as a function of the three rotation angles ϕ, θ and ψ about respective body coordinate system axes. This is written as (Engin & Moeinzadeh, 1983):

$$T = T\,(\theta\,,\,\phi\,,\,\psi) \tag{5}$$

but the order of the rotation angles should be defined as (Shabana, 1989):

$$T = T\,(\phi\,,\,\theta\,,\,\psi) \tag{6}$$

this discrepancy is probably caused by a mistype in (5).

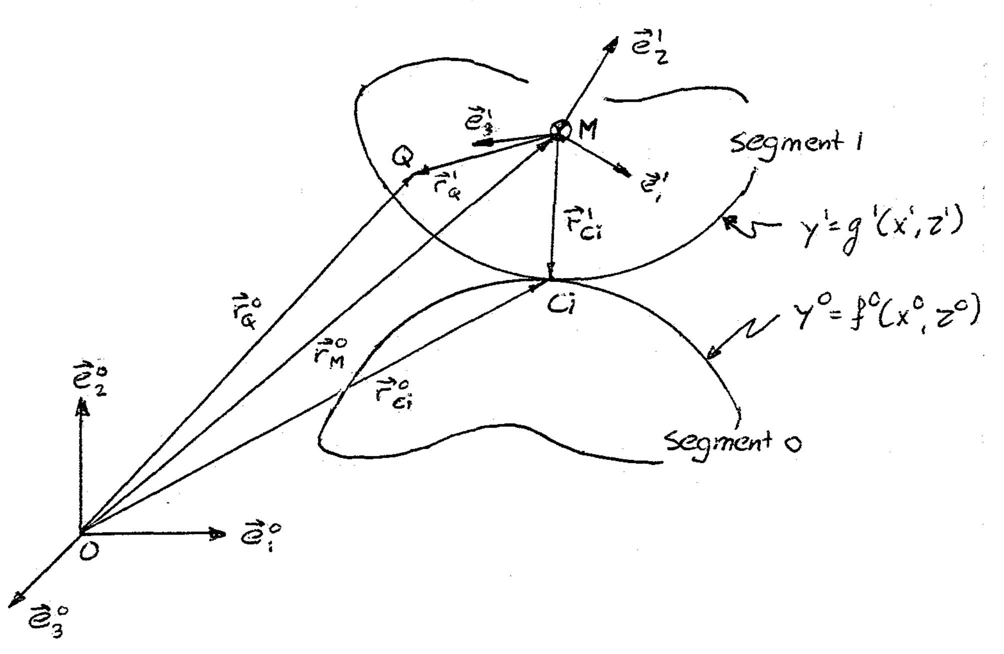

Figure 1. Two-body segmented joint in the 3-dimensional formulation

Moeinzadeh uses a 3-1-3 Euler angle sequence to specify the components of the transformation matrix. It should be noted that this choice is not trivial as for example Wismans (1980) used Bryant angles. More recent developments in the description of the transformation matrix include a joint coordinate system proposed by Grood et al. (1983), in which the system consists of a fixed axis on the fixed body segment, a fixed axis on the moving body segment and a floating axis perpendicular to these two fixed axes, and the use of helical axes (Woltring, 1990 and Karlsson et al., 1991).

When 3-1-3 Euler angle sequence is used, the orientation of the moving coordinate system $(\vec{e}_1^{\,1},\vec{e}_2^{\,1},\vec{e}_3^{\,1})$ is obtained from the fixed coordinate system $(\vec{e}_1^{\,0},\vec{e}_2^{\,0},\vec{e}_3^{\,0})$ by applying successive rotation angles ϕ, θ and ψ (Figure 2). First the $(\vec{e}_1^{\,0},\vec{e}_2^{\,0},\vec{e}_3^{\,0})$ coordinate system is rotated through an angle ϕ about the $\vec{e}_3^{\,0}$ axis of the fixed body coordinate system (Figure 2.a), which results in the intermediary system $(\vec{e}_1^{\,01},\vec{e}_2^{\,01},\vec{e}_3^{\,01})$. The subsequent rotation through an angle θ about the $\vec{e}_1^{\,01}$ axis (Figure 2.b) results in the intermediary system $(\vec{e}_1^{\,02},\vec{e}_1^{\,02},\vec{e}_1^{\,02})$. The final rotation through an angle ψ about the $\vec{e}_3^{\,02}$ (Figure 2.c) gives the orientation of the moving body coordinate system $(\vec{e}_1^{\,1},\vec{e}_2^{\,1},\vec{e}_3^{\,1})$. The orthogonal transformation matrix resulting from the successive rotations is defined as (Engin et al., 1983):

$$\underline{r}^1_M = [\,\underline{T}\,]\underline{r}^0_M \tag{7}$$

with:

$$[\underline{T}] = \begin{bmatrix} \cos\phi\cos\psi-\cos\theta\sin\phi\sin\psi & \sin\phi\cos\psi+\cos\theta\cos\phi\sin\psi & \sin\theta\sin\psi \\ -\cos\phi\sin\psi-\cos\theta\sin\phi\cos\psi & -\sin\phi\sin\psi+\cos\theta\cos\phi\cos\psi & \sin\theta\cos\psi \\ \sin\theta\sin\phi & -\sin\theta\cos\phi & \cos\theta \end{bmatrix} \tag{8}$$

(note that this is the transpose of the transformation matrix as defined by Shabana (1989)).

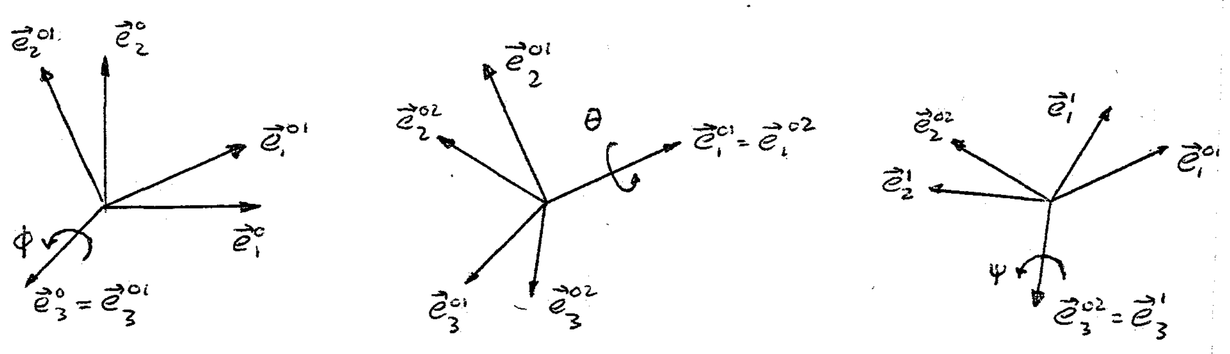

Figure 2. Successive rotations of Euler angles to build the transformation matrix

2.3 Contact Conditions

A rigid body contact between the two body segments at contact points Ci (i is the number of contact points) is assumed (Figure 1). The contact surfaces of the fixed and moving body segments respectively can then be represented by the following continuous functions:

$$y^0 = f^0(x^0, z^0) \tag{9}$$

$$y^1 = g^1(x^1, z^1) \tag{10}$$

The position vectors of the contact points Ci in the bases of the respective body segments are:

$$\vec{r}^{\,0}_{Ci} = x^0_{Ci}\,\vec{e}^{\,0}_1 + f^0(x^0_{Ci}, z^0_{Ci})\,\vec{e}^{\,0}_2 + z^0_{Ci}\,\vec{e}^{\,0}_3 \tag{11}$$

$$\vec{r}^{\,1}_{Ci} = x^1_{Ci}\,\vec{e}^{\,1}_1 + g^1(x^1_{Ci}, z^1_{Ci})\,\vec{e}^{\,1}_2 + z^1_{Ci}\,\vec{e}^{\,1}_3 \tag{12}$$

In analogy to (4), the following contact condition relationship must hold in Ci:

$$\underline{r}^{\,0}_{Ci} = \underline{r}^{\,0}_{M} + [\,\underline{T}\,]^T \underline{r}^{\,1}_{Ci} \tag{13}$$

2.4 Geometric Compatibility

To exclude the possibility of penetration or overlap between the articulating surfaces, it was defined that only a single tangent to both articulating surfaces exist at the contact point. The unit normals to the surfaces of the moving and fixed body segments at the points of contact are therefore colinear to maintain rigid contact. Let $\vec{n}_{Ci}^{\,0}$ be the unit outward normal to the surface of the fixed body segment at points Ci then:

$$\vec{n}^{\,0}_{Ci} = \frac{1}{\sqrt{\det[\underline{G}]}}\left(\frac{\partial \vec{r}^{\,0}_{Ci}}{\partial x^0_{Ci}}\right) \times \left(\frac{\partial \vec{r}^{\,0}_{Ci}}{\partial z^0_{Ci}}\right) \tag{14}$$

where the numerator indicates the direction of the unit outward normal which is determined through the vector product of the articular surface tangents and the denominator normalizes the outward normal to a unit length. The vector $\vec{r}_{Ci}^{\,0}$ is given in (11) and the components of the matrix $[\,\underline{G}\,]$ are determined from:

$$G_{kl} = \left(\frac{\partial \vec{r}^{\,0}_{Ci}}{\partial x^k} \cdot \frac{\partial \vec{r}^{\,0}_{Ci}}{\partial x^l}\right) \quad \text{with kl as matrixcomponents} \tag{15}$$

with:

$$x^1 = x^0_{Ci}\,,\; x^2 = z^0_{Ci}$$

The components of matrix $[\,\underline{G}\,]$ may therefore be written as:

$$G_{xx} = \left[\left(\frac{\partial x^0_{Ci}}{\partial x^0_{Ci}}\right)^2 + \left(\frac{\partial y^0_{Ci}}{\partial x^0_{Ci}}\right)^2 + \left(\frac{\partial z^0_{Ci}}{\partial x^0_{Ci}}\right)^2\right] \tag{16a}$$

$$G_{zz} = \left[\left(\frac{\partial x_{Ci}^0}{\partial z_{Ci}^0}\right)^2 + \left(\frac{\partial y_{Ci}^0}{\partial z_{Ci}^0}\right)^2 + \left(\frac{\partial z_{Ci}^0}{\partial z_{Ci}^0}\right)^2 \right] \tag{16b}$$

$$G_{xz} = G_{zx} = \left[\left(\frac{\partial x_{Ci}^0}{\partial x_{Ci}^0}\right)\left(\frac{\partial x_{Ci}^0}{\partial z_{Ci}^0}\right) + \left(\frac{\partial y_{Ci}^0}{\partial x_{Ci}^0}\right)\left(\frac{\partial y_{Ci}^0}{\partial z_{Ci}^0}\right) + \left(\frac{\partial z_{Ci}^0}{\partial x_{Ci}^0}\right)\left(\frac{\partial z_{Ci}^0}{\partial z_{Ci}^0}\right) \right] \tag{16c}$$

Since $(\partial z_{Ci}^0/\partial x_{Ci}^0)=0$ and $(\partial x_{Ci}^0/\partial z_{Ci}^0)=0$, after substitution the components of matrix [$\underline{G}$] are reduced to:

$$G_{xx} = 1 + \left(\frac{\partial f^0}{\partial x_{Ci}^0}\right)^2 \tag{17a}$$

$$G_{zz} = 1 + \left(\frac{\partial f^0}{\partial z_{Ci}^0}\right)^2 \tag{17b}$$

$$G_{xz} = G_{zx} = \left(\frac{\partial f^0}{\partial x_{Ci}^0}\right)\left(\frac{\partial f^0}{\partial z_{Ci}^0}\right) \tag{17c}$$

From equations (17) the det[$\underline{G}$] can be written as:

$$\det[\underline{G}] = 1 + \left(\frac{\partial f^0}{\partial x_{Ci}^0}\right)^2 + \left(\frac{\partial f^0}{\partial z_{Ci}^0}\right)^2 \tag{18}$$

Furthermore it holds that:

$$\frac{\partial \vec{r}_{Ci}^{\,0}}{\partial x_{Ci}^0} = \vec{e}_1^{\,0} + \frac{\partial f^0}{\partial x_{Ci}^0}\vec{e}_2^{\,0} \tag{19}$$

$$\frac{\partial \vec{r}_{Ci}^{\,0}}{\partial z_{Ci}^0} = \frac{\partial f^0}{\partial z_{Ci}^0}\vec{e}_2^{\,0} + \vec{e}_3^{\,0} \tag{20}$$

$$\left(\frac{\partial \vec{r}_{Ci}^{\,0}}{\partial x_{Ci}^0}\right) \times \left(\frac{\partial \vec{r}_{Ci}^{\,0}}{\partial z_{Ci}^0}\right) = \left(\frac{\partial f^0}{\partial x_{Ci}^0}\right) \vec{e}_1^{\,0} - \vec{e}_2^{\,0} + \left(\frac{\partial f^0}{\partial z_{Ci}^0}\right) \vec{e}_3^{\,0} \tag{21}$$

and therefore the unit outward normal expressed in (14) will have the following form:

$$\vec{n}_{Ci}^{0} = \frac{\gamma}{\sqrt{1 + (\frac{\partial f^0}{\partial x_{Ci}^0})^2 + (\frac{\partial f^0}{\partial z_{Ci}^0})^2}} \left[(\frac{\partial f^0}{\partial x_{Ci}^0})\, \vec{e}_1^{\,0} - \vec{e}_2^{\,0} + (\frac{\partial f^0}{\partial z_{Ci}^0})\, \vec{e}_3^{\,0} \right] \tag{22}$$

where the parameter γ (γ is either +1 or -1) is chosen such that $\vec{n}_{Ci}{}^0$ represents the outward normal. Similarly, following the same procedure as outlined above $\vec{n}_{Ci}{}^1$, the unit outward normal to the moving surface, $y^1=g^1(x^1,z^1)$, at contact points Ci, expressed in the moving body coordinate system can be written as:

$$\vec{n}_{Ci}^{1} = \frac{\beta}{\sqrt{1 + (\frac{\partial g^1}{\partial x_{Ci}^1})^2 + (\frac{\partial g^1}{\partial z_{Ci}^1})^2}} \left[(\frac{\partial g^1}{\partial x_{Ci}^1})\, \vec{e}_1^{\,1} - \vec{e}_2^{\,1} + (\frac{\partial g^1}{\partial z_{Ci}^1})\, \vec{e}_3^{\,1} \right] \tag{23}$$

where the parameter β (β is either +1 or -1) is chosen such that $\vec{n}_{Ci}{}^1$ represents the outward normal. Colinearity of unit normals at each contact point Ci, requires that:

$$\underline{n}_{Ci}^{0} = -[\ \underline{T}\ ]^T \underline{n}_{Ci}^{1} \tag{24}$$

This colinearity condition is also satisfied by requiring that $(\vec{n}_{Ci}{}^0 x T^T \vec{n}_{Ci}{}^1)=\vec{0}$.

In conclusion the contact conditions and geometric compatibility conditions are specified as:

$$\underline{r}_{Ci}^{\,0} = \underline{r}_{M}^{\,0} + [\ \underline{T}\ ]^T \underline{r}_{Ci}^{\,1} \tag{13}$$

$$\underline{n}_{Ci}^{0} = -[\ \underline{T}\ ]^T \underline{n}_{Ci}^{1}. \tag{24}$$

2.5 Ligament Forces

During its motion the moving body segment is subjected to the ligament forces, contact forces and the externally applied forces and moments (Figure 3). The external forces and moments are specified while the contact forces and the ligament forces are unknown and need to be solved from the differential equations which will be discussed in detail in the forthcoming sections.

The ligaments are modelled as nonlinear elastic springs. In the application of the dynamics of the human knee joint, the following force-elongation relationship can be assumed for the major ligaments (the subscript j denotes the jth ligament):

$$\vec{F}_j^{\,0} = F_j \vec{\lambda}_j^{\,0} \tag{25}$$

in which F_j gives a specific constitutive relation and $\vec{\lambda}_j{}^0$ denotes the ligament unit vector. Let $\vec{r}_{j1}{}^1$ be the position vector of the primary insertion point of the ligament j in the moving body segment. The position vector of the secundary insertion point of the same ligament j in the fixed body segment is denoted by $\vec{r}_{j0}{}^0$. The subscripts m and f outside the parenthesis imply "moving" and fixed", respectively.

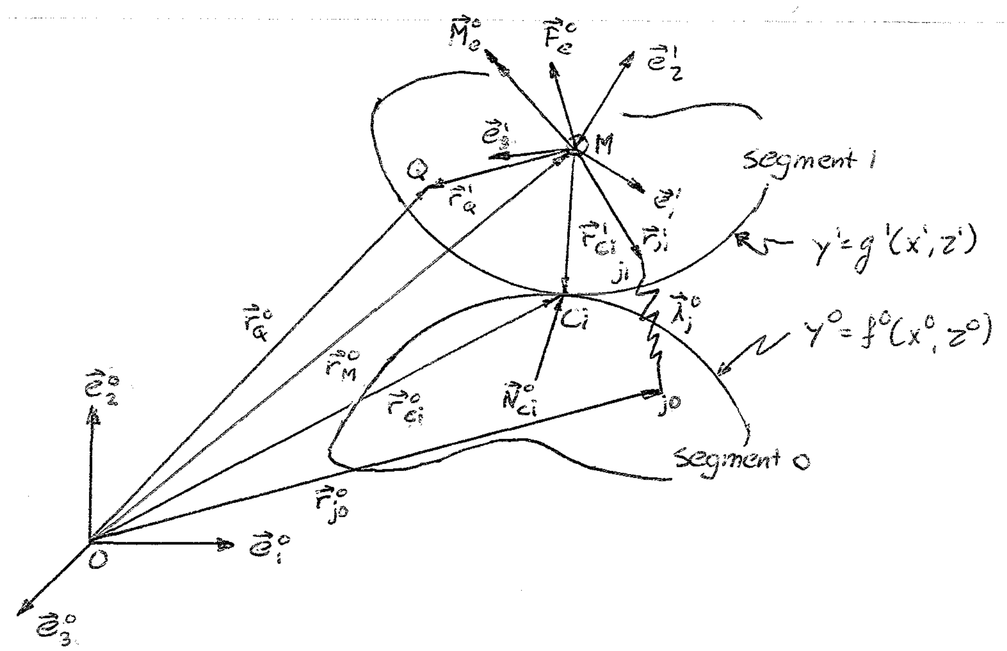

Figure 3. Human articulating joint with force descriptions

The unit vector $\vec{\lambda}_j^0$ along the ligament j directed from the moving body insertion point j1 to the fixed body segment origin point j0 is:

$$\vec{\lambda}_j^0 = \frac{1}{L_j}[\vec{r}_{j0}^0 - \vec{r}_M^0 - [\,T^T\,]\vec{r}_{j1}^1] \tag{26}$$

in which the current length of the ligament is given by:

$$L_j = \sqrt{[\vec{r}_{j0}^0 - \vec{r}_M^0 - [\,T^T\,]\vec{r}_{j1}^1] \cdot [\vec{r}_{j0}^0 - \vec{r}_M^0 - [\,T^T\,]\vec{r}_{j1}^1]} \tag{27}$$

2.6 Contact Forces

The friction force between the moving and the fixed body segments is considered negligible. Due to the contact between the articulating surfaces, the fixed body segment exerts a force on the moving body segment as it moves along its articulating surface. The contact force will be in the direction of the outward normal of the surface in the contact point Ci. The contact forces $\vec{N}_{Ci}^0$ in the contact points acting on the moving body segment are given by:

$$\vec{N}_{Ci}^0 = |N_{Ci}^0|[(n_{Ci}^0)_x\vec{e}_1^0 + (n_{Ci}^0)_y\vec{e}_2^0 + (n_{Ci}^0)_z\vec{e}_3^0] \tag{28}$$

where $|N_{Ci}^0|$ is the unknown magnitude of the contact forces and $(n_{Ci}^0)_x$, $(n_{Ci}^0)_y$ and $(n_{Ci}^0)_z$ are the components of the unit normal $\vec{n}_{Ci}^0$ in the x,y and z directions of the fixed body coordinate system respectively.

2.7 External Forces and Moments

The moving body segment of the joint can be subjected to various external forces (gravitational force, forcing pulse, muscle forces or accelerations applied directly to the bones outside the articular area). The external moment vector can consist of applied external moments (e.g. prescribed torques) and the moments caused by the external forces. The resultants of the external forces and moments at the center of mass of the moving body segment are given as:

$$F_e^0 = (F_e^0)_x\vec{e}_1^{\,0} + (F_e^0)_y\vec{e}_2^{\,0} + (F_e^0)_z\vec{e}_3^{\,0} \tag{29}$$

$$M_e^0 = (M_e^0)_x\vec{e}_1^{\,0} + (M_e^0)_y\vec{e}_2^{\,0} + (M_e^0)_z\vec{e}_3^{\,0} \tag{30}$$

2.8 Equations of motion

The equations governing the motion of the moving body segment given in the fixed body coordinate system as function of the applied forced and moments are:

$$(F_e^0)_x + \sum_{i=1}^{q} |N_{Ci}^0|(n_{Ci}^0)_x + \sum_{j=1}^{p} F_j(\lambda_j^0)_x = m\ddot{x}_M^0 \tag{31a}$$

$$(F_e^0)_y + \sum_{i=1}^{q} |N_{Ci}^0|(n_{Ci}^0)_y + \sum_{j=1}^{p} F_j(\lambda_j^0)_y = m\ddot{y}_M^0 \tag{31b}$$

$$(F_e^0)_z + \sum_{i=1}^{q} |N_{Ci}^0|(n_{Ci}^0)_z + \sum_{j=1}^{p} F_j(\lambda_j^0)_z = m\ddot{z}_M^0 \tag{31c}$$

$$\sum M_{x^1x^1}^0 = I_{x^1x^1}\dot{\omega}_{x^1} + (I_{z^1z^1}-I_{y^1y^1})\omega_{y^1}\omega_{z^1} \tag{32a}$$

$$\sum M_{y^1y^1}^0 = I_{y^1y^1}\dot{\omega}_{y^1} + (I_{x^1x^1}-I_{z^1z^1})\omega_{z^1}\omega_{x^1} \tag{32b}$$

$$\sum M_{z^1z^1}^0 = I_{z^1z^1}\dot{\omega}_{z^1} + (I_{y^1y^1}-I_{x^1x^1})\omega_{x^1}\omega_{y^1} \tag{32c}$$

where $\ddot{x}_M^0$ denotes the second time derivative of the motion in the $\vec{e}_1^{\,0}$ direction, m denotes the mass of the moving body segment, p and q represent the number of ligaments and contact points respectively. $I_{x'x'}$, $I_{y'y'}$ and $I_{z'z'}$ are the principal moments of inertia of the moving body segment about the (x^1,y^1,z^1) axis system and $\omega_{x'}$, $\omega_{y'}$ and $\omega_{z'}$ are the components of the angular velocity vector in terms of the Euler angles (Engin et al., 1983):

$$\omega_{x^1} = \dot{\theta}\cos\psi + \dot{\phi}\sin\theta\sin\psi \tag{33a}$$

$$\omega_{y^1} = \dot{\theta}\sin\psi + \dot{\phi}\sin\theta\cos\psi \tag{33b}$$

$$\omega_{z^1} = \dot{\phi}\cos\theta + \dot{\psi} \tag{33c}$$

The angular acceleration components $\dot{\omega}_{x'}$, $\dot{\omega}_{y'}$ and $\dot{\omega}_{z'}$ are directly obtained from the time derivatives of the previous equations:

$$\dot{\omega}_{x_1} = \ddot{\theta}\cos\psi - \dot{\psi}(\dot{\theta}\sin\psi - \dot{\phi}\cos\psi\sin\theta) + \ddot{\phi}\sin\theta\sin\psi + \dot{\phi}\dot{\theta}\cos\theta\sin\psi \tag{34a}$$

$$\dot{\omega}_{y_1} = -\ddot{\theta}\sin\psi - \dot{\psi}(\dot{\theta}\cos\psi - \dot{\phi}\sin\psi\sin\theta) + \ddot{\phi}\sin\theta\cos\psi + \dot{\phi}\dot{\theta}\cos\theta\cos\psi \tag{34b}$$

$$\dot{\omega}_{z^1} = \ddot{\phi}\cos\theta - \dot{\phi}\dot{\theta}\sin\theta + \ddot{\psi} \tag{34c}$$

Note that the moment components on the left-hand side of (32) have the following terms:

$$\vec{M}^0 = \vec{M}_e^0 + \sum_{i=1}^{q} [\underline{T}]^T(\vec{r}_{Ci}^1)x(|N_{Ci}^0|\vec{n}_{Ci}^0) + \sum_{j=1}^{p} [\underline{T}]^T(\vec{r}_{j1}^1)x(F_j\vec{\lambda}_j^0) \tag{35}$$

Equations (31) and (32) form a set of 6 nonlinear second-order differential equations which together with the contact and geometric compatibility conditions:

$$\underline{r}_{Ci}^0 = \underline{r}_M^0 + [\,\underline{T}\,]^T\underline{r}_{Ci}^1 \tag{13}$$

$$\underline{n}_{Ci}^0 = -[\,\underline{T}\,]^T\underline{n}_{Ci}^1 \tag{24}$$

result in a set of 16 nonlinear equations with 16 unknowns (if 2 contact points are considered):
(a) ϕ, θ and ψ which determine the time-dependent components of transformation matrix [T]
(b) x_M^0, y_M^0 and z_M^0: the components of position vector $\vec{r}_M^0$
(c) x_{C1}^0, z_{C1}^0, x_{C1}^1, z_{C1}^1, x_{C2}^0, z_{C2}^0, x_{C2}^1, z_{C2}^1: the coordinates of the contact points
(d) $|N_{C1}^0|$, $|N_{C2}^0|$: the magnitudes of the contact forces in the contact points
The problem is completed by prescribing initial conditions at t=0:

$$\dot{x}_M^0 = \dot{y}_M^0 = \dot{z}_M^0 = 0 \tag{36a}$$

$$\omega_x = \omega_y = \omega_z = 0 \tag{36b}$$

along with specified values for x_M^0, y_M^0, z_M^0, ϕ, θ and ψ. The numerical procedures which can be used to solve the system of equations will be described in the following chapter.

The following observations can be made: during its motion the moving body segment is subjected to unknown ligament forces, contact forces, and specified applied forces and moments (Figure 3). The model is intended to simulate events which take place during a very short time period such as 0.1 seconds. Engin et al. (1985) state that the muscle forces need therefore not be included in the dynamic modelling of an articulating joint because it is sufficient to consider only the passive resisitive forces at the model formulation. Recent research (Thunnissen, 1993) has on the other hand indicated that there are muscles in for example the human lower limbs that have sufficiently short reaction times to be able to contribute to the forces in the equations of motion (31) & (32). Direct exclusion of the muscle forces from the current model does not restrict its capabilities to have the effects of muscle forces to be included as a part of the applied force and moment vector on the moving body segment (Engin et al., 1985). Another option is to directly implement the muscle forces into the model, comparable to the manner in which the ligament forces are implemented. Tümer & Engin (1993) described a three-body segment dynamic model of the human knee which enables one to obtain the dynamic response of the knee joint to muscle actions (quadriceps, femoris, hamstrings and gastrocnemicus) as well as externally applied forces.

3. Numerical Procedure

3.1 Introduction

The mathematical formulation which has been described in the previous chapter has in literature mainly been applied to the description of the motion of the human knee (primarily the articulating joint connecting the femur and tibia excluding the patella) as a result of external forces. Due to the fact that the 3-dimensional formulation is more extensive and an efficient numerical procedure has not yet been found, the applications focus on the motion of the knee in the 2-dimensional sagittal plane.

In this chapter, the numerical solution procedure which was initially discussed by Moeinzadeh (1981) and Engin and Moeinzadeh (1983) will firstly be discussed. It can be concluded that this numerical procedure is not efficient and several alternative solution methods which have appeared in literature (e.g. method of excess differential equations and method of minimal differential equations) will be briefly compared to the original numerical procedure. It must be noted that it is not within the scope of this report to extensively discuss each numerical solution technique. In Chapter 4, the numerical solution will be discussed in more detail when the modelling technique is applied to a 2-dimensional human knee. Finally, the applicability of the classical impact theory will be discussed and conclusions can be drawn.

3.2 Numerical Solution Technique as Proposed by Engin and Moeinzadeh

As mentioned in the previous section, a 2-dimensional model of the human knee with one contact point is regarded. The governing equations of the initial value problem are the 3 equations of motion (31) and (32), 2 contact conditions (13) and 1 geometric compatibility condition (24). The problem is thus reduced to the solution of a set of 6 simultaneous nonlinear differential and algebraic equations. The unknowns of the problem are x_M^0, y_M^0, ϕ, x_{CI}^0, x_{CI}^1, and $|N_{CI}^0|$.

Engin & Moeinzadeh (1983) and Abdel-Rahman & Hefzy (1993) propose the use of Newmark operators to replace the time derivatives of the unknown variables of (31) and (32) with a temporal operator in order to obtain a numerical solution. The Newmark method divides the time span of motion into small time increments Δt and assumes that the second time derivative over each time increment is constant. For example, the acceleration $\ddot{x}_M^0$ at time point t can be expressed in the following form:

$$(\ddot{x}_M^0)^t = \frac{4}{(\Delta t)^2}[(x_M^0)^t - (x_M^0)^{t-\Delta t}] - \frac{4}{\Delta t}(\dot{x}_M^0)^{t-\Delta t} - (\ddot{x}_M^0)^{t-\Delta t} \tag{37a}$$

in which the superscripts refer to the time points. Similar expressions may be used to determine the other time dependent acceleration components of (31) and (32). In the applications, the initial conditions at t=0 and subsequent conditions at the previous time point (t-Δt) are assumed to be known. Using (37a), the acceleration at time point t can thus be determined in terms of the position at time points t and t-Δt, the velocity and acceleration at time point t-Δt.

The velocity at time point t can be determined in terms of the velocity and acceleration at time point t-Δt and the acceleration at time point t:

$$(\dot{x}_M^0)^t = (\dot{x}_M^0)^{t-\Delta t} + \frac{\Delta t}{2}[(\ddot{x}_M^0)^{t-\Delta t} + (\ddot{x}_M^0)^t] \tag{37b}$$

After the time derivatives in (31) and (32) are replaced with the temporal operators (37a) and (37b), the governing equations take the form of a set of nonlinear algebraic equations. The solution of these equations is complicated by the fact that iteration or perturbation methods must be used. The Newton-Raphson iteration process can be used to obtain a solution. In the derivation of the linearized equations of motion, the following assumption is made:

$$(x_M^0)_k^t = (x_M^0)_{k-1}^t + (\Delta x_M^0)_k \qquad (38)$$

in which the Δ quantities denote incremental values and the subscripts denote iteration steps. Knowledge of the variables of the previous iteration (k-1) is hereby essential at each iteration number k. Equation (38) can be applied to the other variables which in addition to the independent variables also include the components of the insertion points and normals. The variables are substituted into the governing nonlinear algebraic equations and the higher order terms in the Δ quantities are neglected. This results in a set of 22 simultaneous algebraic equations which can be put into the following matrix form:

$$[\underline{K}]\underline{\Delta} = \underline{D} \qquad (39)$$

where [$\underline{K}$] is a 22x22 coefficient matrix, $\underline{\Delta}$ is a vector of incremental quantities and $\underline{D}$ is a vector of known values.

The iteration process at a fixed time point continues until the Δ quantities of all the variables satisfy a prescribed convergence criterion. In (Engin et al., 1983), a solution is accepted and iteration process is terminated when the Δ quantities become less than 0.01% of the previous values of the corresponding variables. The converged solution of each variable is then used as the initial value for the next time step and the process is repeated for consecutive time steps.

The numerical solution scheme requires very short time increments to be used to achieve convergence especially when time duration of applied forces is small. In this case it becomes necessary to use very small time steps otherwise a significantly large number of iterations is required for convergence. The upper limit of the value of the time increment is chosen such that the accuracy of the solution and convergence of the Newton-Raphson iteration is guaranteed. A lower limit is chosen in order to maintain stability because a smaller value of Δt increases the ill-conditioning of the stiffness matrix. An indication of the value of the time increment is given by Engin & Moeinzadeh (1983) who used as time increment of Δt=0.0001 seconds during a simulation time span of 0.36 seconds.

The current solution technique cannot handle impact type external loads and the solution technique presents problems when the moving body segment changes its direction of motion under the action of the pulling force of the ligaments. The current solution technique only yields results for the extension phase of the knee motion and can not continue to cover the rotation of the tibia relative to the femur due to the pulling force of the ligaments upon removal of the external forcing pulse (Engin and Tümer, 1993).

3.3 Introduction of Alternative Solution Methods

The governing equations for the articulating joint model described in the previous sections are in the form of three second-order nonlinear differential equations coupled with nonlinear algebraic equations of geometric constraints. The method of solution constitues replacing the time derivatives in the differential equations by a temporal operator and solving the resulting set of algebraic equations by iteration at every fixed time point.

In this section several alternative solution methods to solve the governing equations are discussed and compared. The solution methods are:

- method of excess differential equations

- method of minimal differential equations

3.4 Method of Excess Differential Equations (EDE)

In the application of the method of excess differential equations (Engin and Tümer, 1991 & 1993), the constraint equations are differentiated twice and the resulting second-order simultaneous differential equations can be numerically integrated using for example Euler of Runge-Kutta integration schemes. The basic postulate of this approach is that if the constraints are satisfied initially, then satisfying the second derivatives of the constraints in future time steps would also satisfy the constraints themselves.

The 2-dimensional situation will be focused on for reasons of simplicity. Upon differentiating the contact conditions twice, a set of 6 coupled second order differential equations is obtained which can be arranged into the following matrix form:

$$[A]\left[\ddot{x}_M^0 \;\; \ddot{y}_M^0 \;\; \ddot{\theta} \;\; \ddot{x}_{C1}^0 \;\; \ddot{x}_{C1}^1 \;\; N_{C1}^0\right]^T = [F_1 \;,\; . \; . \; . \; . \;,\; F_6]^T \tag{40}$$

where [A] is a 6x6 configuration-dependent coefficient matrix and $[F_1,...,F_6]^T$ is a configuration and time-dependent forcing column vector. The unknown vector of accelerations and contact force can then be solved:

$$\left[\ddot{x}_M^0 \;\; \ddot{y}_M^0 \;\; \ddot{\theta} \;\; \ddot{x}_{C1}^0 \;\; \ddot{x}_{C1}^1\right]^T = [S_1 \;,\; . \; . \; . \;,\; S_5]^T \quad \text{and} \quad N_{C1}^0 = S_6 \tag{41}$$

where S_i are the elements of the vector $[A]^{-1}[F]^T$ and are expressed in terms of 5 position variables (x_M^0, y_M^0, θ, x_{C1}^0, x_{C1}^1), their first derivatives and the specified external forces. Knowing the position variables and their derivatives at the previous time point, the first part of (41) can be numerically integrated to find position variables and their first derivatives at the current time. The corresponding contact force can then be found from the second part of (41). The integration process can be repeated as many times as required until the total simulation time is reached. This method involves far less mathematical manipulation than the previous method (section 3.2) and the numerical solution is restricted to the integration process and does not require iteration.

3.5 Method of Minimal Differential Equations (MDE)

The method of minimal differential equations (Engin and Tümer, 1991 & 1993) aims at reducing the number of differential equations in closed form by satisfying constraint equations as well as their derivations and solving only the resulting nonlinear differential equations via numerical integration. The aim would be to have a minimum number of simultaneous differential equations describing the dynamics of a system. Since the number of degrees of freedom of the 2-dimensional human knee is 2, its dynamics can in principal be expressed by two differential equations in terms of 2 appropriately chosen generalized coordinates. For the human knee, x_{C1}^0 and ϕ (rotation about the axis perpendicular to the plane of motion) are chosen as the generalized coordinates.

Since (13) are linear in terms of velocity variables, it is possible to express $\dot{x}_M^0$ and $\dot{y}_M^0$ as linear combinations of the generalized coordinates:

$$\dot{x}_M^0 = \lambda_\phi \dot{\phi} + \lambda_x \dot{x}_{C1}^0 \tag{42a}$$

The acceleration components of the origin of the moving body segment can then be expressed as:
in which the definitions for λ_k and μ_k (k=ϕ,x,d) can be found in (Engin and Tümer, 1991) and

$$\dot{y}_M^0 = \mu_\phi \dot{\phi} + \mu_x \dot{x}_{C1}^0 \tag{42b}$$

$$\ddot{x}_M^0 = \lambda_\phi \ddot{\phi} + \lambda_x \ddot{x}_{C1}^0 + \lambda_d \tag{43a}$$

$$\ddot{y}_M^0 = \mu_\phi \ddot{\phi} + \mu_x \ddot{x}_{C1}^0 + \mu_d \tag{43b}$$

(Engin and Tümer, 1993). We can arrange the original differential equations (32)-(33) into the following form by using elements of matrix [A] and vector $[F]^T$ given in (41):

$$a_{11} \ddot{x}_M^0 + a_{16} N_{C1}^0 = F_1 \tag{44a}$$

$$a_{22} \ddot{y}_M^0 + a_{26} N_{C1}^0 = F_2 \tag{44b}$$

$$a_{33} \ddot{\phi} + a_{36} N_{C1}^0 = F_3 \tag{44c}$$

We then solve for N^0_{C1} from the previous equation and substitute into the (44a) and (44b) together with (42) and thus obtain:

$$[B][\ddot{\phi} \;\; \ddot{x}_{C1}^0]^T = [H_1 \;\; H_2]^T \tag{45}$$

where [B] is a 2x2 configuration-dependent coefficient matrix and $[H]^T$ is a configuration- and time-dependent forcing vector. (45) can now be integrated to obtain the dynamic response in terms of the generalized coordinates ϕ and $x_{C1}{}^0$. The contact force N^0_{C1} is directly found from (44c). It is necessary to solve the geometric constraint equations after every integration time step in order to be able to proceed on with the next step. The nature of the constraint equations (13) allows one to obtain closed form expressions for $x_M{}^0$, $y_M{}^0$, and $y_{C1}{}^1$ in terms of the generalized coordinates ϕ and $x_{C1}{}^0$.

3.6 Comparison of the EDE and MDE Methods

The EDE and MDE methods are in principal mathematically equivalent. In fact after a series of row operations on matrix (40) it can be shown that (45) is a partitioned form of (41). From a numerical solution point of view however, these methods are not equivalent. The MDE method is considered to be more reliable since the constraints are directly satisfied at every integration step whereas in the EDE method, the constraints are directly satisfied only at the inital time point.The advantages of the EDE formulation include a straightforward approach and simple application of any problem of this kind. The MDE method firstly requires a proper choice of generalized coordinates and even then it might not always be possible to arrive at the desired formulation. For more complicated problems, when for example a 3-dimensional model of the human knee is regarded, the straightforward application of the EDE method may prove to be a suitable alternative when used together with a reliable integration scheme instead of the less feasible MDE method.

Both the EDE and MDE methods were programmed in quick basic by utilizing the Euler and fourth-order Runge-Kutta integration schemes (Engin and Tümer, 1991 & 1993). Results showed that as the bulk of the calculations are essentially the same, formulations of the EDE and MDE methods take practically the same time (execution time in the order of 1-3 minutes on an IBM-PC system 2 for a simulation time of 0.15s) and yield stable results. The Runge-Kutta integration scheme requires considerable more time than the Euler integration but is considered to be a more sophisticated and accurate. If minimal computational effort is required then the combination of the MDE method and Euler integration scheme is the optimal combination.

If one considers the iterative nature of the numerical procedure described in section 3.2 then, superiority of the EDE and MDE methods may comfortable be claimed for both accuracy and efficiency. Furthermore all shortcomings of the previous iterative method of solution are eliminated by the alternative methods.

3.7 Solution Procedure Proposed by Abdel-Rahman

Abdel-Rahman (Abdel-Rahman & Hefzy, 1993) adopt an analysis in which the reverse of the EDE method is used by transforming the differential equations of motion into three algebraic equations using a Newmark method. A differential form of the Newton-Raphson method is then used to solve these algebraic nonlinear equations. This method basically consists of differentiating the system of equations with respect to the independent variables, solving thus an equal amount of equations in an equal amount of unknowns.

The main difference between the solution procedure which was described in section 3.2 which also used a Newton-Raphson solution method is that now the equations are only differentiated to the 6 independent variables instead of additonal dependent variables. It is difficult to conclude if this method is more efficient than the EDE or MDE methods and an in depth implementation of the mentioned methods in the application of the 2-dimensional knee is required.

3.8 Application of the Classic Impact Theory

The numerical solution procedure (section 3.2) adopted very small time increments to be used to achieve convergence: the solution technique could therefore not handle impact type external loads in which the time duration of applied forces is very short. The results presented for the 2-dimensional model of the knee joint have been restricted to short time intervals during which response is smooth and free from abrupt changes.

The applicability of the classic impact theory was examined by Engin and Tümer (1992 & 1993) by taking the 2-dimensional human knee joint as an example. The EDE and MDE methods are used to obtain the response of the human knee joint to impact loading on the lower leg via an anatomically-based model. The classic impact theory is applied to the same model and results in an approximate solution. By comparing both solutions, applicability of the classical impact theory to an anatomically based joint model will be investigated and its shortcomings will be delineated.

The classical impact theory is based on the assumption that impact duration is sufficiently short to allow the following simplifications to be made:

- geometry does not change during impact
- time integrals of finite quantities over the duration of the impact are negligible

To apply the impact theory to the present model, the equations of motion are first integrated from $t=0$ to $t=\tau$, where τ is the impact period. With the above-mentioned assumptions of the impact theory, the equations are simplified and put in following form:

$$m\Delta\dot{x}_M^0 + a_{16}S_N = S_x \tag{46a}$$

where Δ indicates a change in velocity terms, S_N,S_x, S_y and H are impulses of the contact force,

$$m\Delta\dot{y}_M^0 + a_{26}S_N = S_y \tag{46b}$$

$$I\Delta\dot{\theta} + a_{36}S_N = H \tag{46c}$$

external force and external moment respectively. The coefficients are defined as in (40). After substituting (42a) and (42b) in (46), the values for S_N and $\dot{\theta}$ can then be found using matrix algebra.

The effects of the lower leg inertia (mass m and inertia I) and externally applied pulse (S_x, S_y, H) and knee configuration at the time of impact can be identified. It should be noted that the geometric terms include the effects of the form of the contact surfaces on the impact phenomenon. This results in the effect that according to the assumptions of the classic impact theory, the ligaments can not sustain any impact since the ligament forces are position dependent.

The results of test simulations establish the fact that the classical impact theory gives the limiting solution to the model equations as the impact time τ approaches zero. Moreover the results indicate inapplicability of the classical impact theory to practical situations where the impact time can range from 15 to 30 ms. Another problem associated with the application of the classical impact theory to the solution of the anatomically based models is the difficulty of interpreting the results obtained in the form of impulses. It has been shown that impulse magnitude alone is not sufficient to assess the loading condition at the joint. The fact that ligament response is not instantaneous entails its exclusion from the classical impact theory; whereas real time simulations have shown that the ligaments are affected by the impact in comparable magnitudes with contact forces.

4. Implementation of a 2-Dimensional Knee Joint Model in MADYMO

4.1 Introduction

In this chapter the numerical procedures which were described in the previous chapter will be regarded more closely. This serves a dual purpose as primarily knowledge of the efficiency of the solution procedures can be gained and in addition, the possibilities of MADYMO (MADYMO Users Manual, 1994) and it's algorithms in providing a solution can also be verified. MADYMO was chosen because first hand programming knowledge and experience were at hand and efficient coupling to algorithm libraries was available.

This Chapter describes the implementation of a dynamic joint model in MADYMO using the modelling technique. The implementation considers the 2-dimensional articulating motion between the femur and the tibia and does not consider the patella. For this purpose, a knee joint model based on available data in the literature is implemented in MADYMO. The 2-dimensional dynamic anatomical model of the human knee joint is modelled as a fixed femur and moving tibia connected by 4 nonlinear springs representing the different ligaments. Forces consisted of a single point contact force and a gravitational force which acts on the tibia. Knee response was determined under sudden rectangular pulsing posterior forces applied to the tibia. To solve the set of nonlinear constraints, a user-subroutine is written. The model is validated with the results of Moeinzadeh et al. (1983).

4.2 Mathematical Formulation

In the review of the dynamic modelling of human articulating joints, it was shown that the contact between two articulating body segments (Figure 4.1) is controlled by contact position condition (contact condition) and contact normal condition (geometric compatibility condition) constraints.

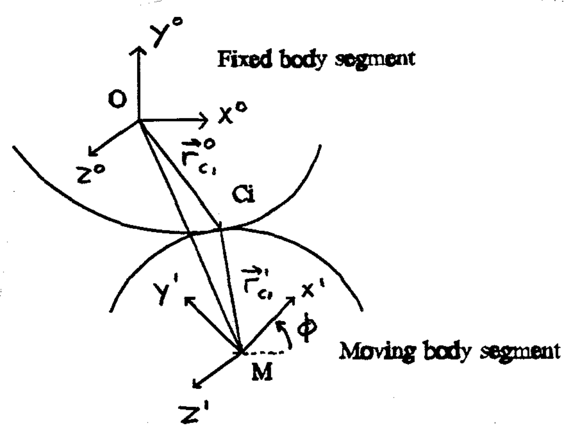

Figure 4.1: Articulating contact between the fixed body segment and the moving body segment

If motion is regarded in the 2-dimensional plane, the system of constraints (13) & (24) narrows down to 3 equations. The 2-dimensional plane is spanned by the x- and y-axes (the z-axis is perpendicular to the plane (Figure 4.1). The system of constarints results in:

$$\begin{bmatrix} x_{C1}^{0} \\ y_{C1}^{0} \end{bmatrix} = \begin{bmatrix} x_{M}^{0} \\ y_{M}^{0} \end{bmatrix} + \underline{T} \begin{bmatrix} x_{C1}^{1} \\ y_{C1}^{1} \end{bmatrix} \tag{47}$$

$$\cos(\phi)\left(\frac{dy_{C1}^{0}}{dx_{C1}^{0}} - \frac{dy_{C1}^{1}}{dx_{C1}^{1}}\right) - \sin(\phi)\left(1 + \frac{dy_{C1}^{0}}{dx_{C1}^{0}}\frac{dy_{C1}^{1}}{dx_{C1}^{1}}\right) = 0 \tag{48}$$

in which $\underline{T}$ transforms the orientation of the moving body segment coordinate system into the fixed body segment coordinate system and is defined as:

$$\underline{T} = \begin{bmatrix} \cos(\phi) & -\sin(\phi) \\ \sin(\phi) & \cos(\phi) \end{bmatrix} \tag{49}$$

The displacement of the moving body segment relative to the fixed body segment in the 2-dimensional plane can be described by two independent parameters. In essence, the method of minimal differential equations is applied. Rewriting the contact position condition results in an equation for the position of the mass center of the moving body segment as function of the independent and dependent coordinates:

$$\begin{bmatrix} x_{M}^{0} \\ y_{M}^{0} \end{bmatrix} = \begin{bmatrix} x_{C1}^{0} - \cos(\phi)x_{C1}^{1} + \sin(\phi)y_{C1}^{1} \\ y_{C1}^{0} - \sin(\phi)x_{C1}^{1} - \cos(\phi)y_{C1}^{1} \end{bmatrix} \tag{50}$$

The independent ($\underline{q}_i$) and dependent joint coordinates ($\underline{q}_d$) are specified as follows:

$$\underline{q}_i = \begin{bmatrix} x_{C1}^{0} \\ \phi \end{bmatrix} , \quad \underline{q}_d = \begin{bmatrix} x_{M}^{0} \\ y_{M}^{0} \\ x_{C1}^{1} \end{bmatrix} \tag{51}$$

The following abbreviations are now introduced, in which n denotes the nth derivative:

$$d^{\,n}y_{C1}^{0} \equiv \frac{d^{\,n}y_{C1}^{0}}{dx_{C1}^{0\;n}} , \quad d^{\,n}y_{C1}^{1} \equiv \frac{d^{\,n}y_{C1}^{1}}{dx_{C1}^{1\;n}} \tag{52}$$

The position formulation of the mass center of the moving body segment can be differentiated with respect to time and this results in the velocity formulation:

$$\begin{bmatrix} \dot{x}_{M}^{0} \\ \dot{y}_{M}^{0} \end{bmatrix} = \begin{bmatrix} 1 & \sin(\phi)x_{C1}^{1} + \cos(\phi)y_{C1}^{1} \\ dy_{C1}^{0} & -\cos(\phi)x_{C1}^{1} + \sin(\phi)y_{C1}^{1} \end{bmatrix} \begin{bmatrix} \dot{x}_{C1}^{0} \\ \dot{\phi} \end{bmatrix} + \begin{bmatrix} -\cos(\phi) + \sin(\phi)dy_{C1}^{1} \\ -\sin(\phi) - \cos(\phi)dy_{C1}^{1} \end{bmatrix} \begin{bmatrix} \dot{x}_{C1}^{1} \end{bmatrix} \tag{53}$$

The aim is to write this formulation as a function of the time derivatives of the independent coordinates. The constraint concerning the contact normal condition (47) can be used for this purpose. The constraint equation is therefor differentiated to time and written as a function of the independent and dependent coordinates:

$$\dot{x}_{C1}^{1} = \frac{1}{d_1}\left[d_2\,\dot{x}_{C1}^{0} + d_3\,\dot{\phi}\right] \tag{54}$$

with the following abbreviations:

$$d_1 = \cos(\phi)d^2y_{C1}^{1} + \sin(\phi)dy_{C1}^{0}d^2y_{C1}^{1} \tag{55}$$

$$d_2 = -\sin(\phi)d^2y_{C1}^{0}dy_{C1}^{1}+\cos(\phi)d^2y_{C1}^{0} \tag{56}$$

$$d_3 = \sin(\phi)(dy_{C1}^{1}-dy_{C1}^{0})-\cos(\phi)(1+dy_{C1}^{0}dy_{C1}^{1}) \tag{57}$$

If the previous equations are substituted in the velocity formulation, this results in:

$$\begin{bmatrix}\dot{x}_M^0\\ \dot{y}_M^0\end{bmatrix} = \begin{bmatrix}1+d_2d_4 & \sin(\phi)x_{C1}^{1}+\cos(\phi)y_{C1}^{1}+d_3d_4\\ dy_{C1}^{0}+d_2d_5 & -\cos(\phi)x_{C1}^{1}+\sin(\phi)y_{C1}^{1}+d_3d_5\end{bmatrix}\begin{bmatrix}\dot{x}_{C1}^{0}\\ \dot{\phi}\end{bmatrix} = \underline{F}\begin{bmatrix}\dot{x}_{C1}^{0}\\ \dot{\phi}\end{bmatrix} \tag{58}$$

with the following abbreviations:

$$d_4 = \frac{-\cos(\phi)+\sin(\phi)dy_{C1}^{1}}{d_1} \tag{59}$$

$$d_5 = \frac{-\sin(\phi)-\cos(\phi)dy_{C1}^{1}}{d_1} \tag{60}$$

The second time derivative of the state formulation can now be derived:

$$\begin{bmatrix}\ddot{x}_M^0\\ \ddot{y}_M^0\end{bmatrix} = \underline{F}\begin{bmatrix}\ddot{x}_{C1}^{0}\\ \ddot{\phi}\end{bmatrix} + \dot{\underline{F}}\begin{bmatrix}\dot{x}_{C1}^{0}\\ \dot{\phi}\end{bmatrix} \tag{61}$$

in which $\dot{\underline{F}}$ is:

$$\dot{\underline{F}} = \begin{bmatrix}\dot{d}_2d_4+d_2\dot{d}_4 & \dot{\phi}\cos(\phi)x_{C1}^{1}+\sin(\phi)\dot{x}_{C1}^{1}-\dot{\phi}\sin(\phi)y_{C1}^{1}+\cos(\phi)dy_{C1}^{1}\dot{x}_{C1}^{1}+\dot{d}_3d_4+d_3\dot{d}_4\\ d^2y_{C1}^{0}\dot{x}_{C1}^{0}+\dot{d}_2d_5+d_2\dot{d}_5 & \dot{\phi}\sin(\phi)x_{C1}^{1}-\cos(\phi)\dot{x}_{C1}^{1}+\dot{\phi}\cos(\phi)y_{C1}^{1}+\sin(\phi)dy_{C1}^{1}\dot{x}_{C1}^{1}+\dot{d}_3d_5+d_3\dot{d}_5\end{bmatrix} \tag{62}$$

with the following abbreviations (in which $\dot{x}_{C1}{}^{1}$ is known as a function of the independent coordinates and their derivatives (54)):

$$\dot{d}_1 = -\dot{\phi}\sin(\phi)d^2y_{C1}^1+\cos(\phi)d^3y_{C1}^1\dot{x}_{C1}^1+\dot{\phi}\cos(\phi)dy_{C1}^0d^2y_{C1}^1+ \\ \sin(\phi)\left[d^2y_{C1}^0d^2y_{C1}^1\dot{x}_{C1}^0+dy_{C1}^0d^3y_{C1}^1\dot{x}_{C1}^1\right] \tag{63}$$

$$\dot{d}_2 = \frac{-\dot{\phi}\cos(\phi)d^2y_{C1}^0dy_{C1}^1-\sin(\phi)(d^3y_{C1}^0dy_{C1}^1\dot{x}_{C1}^0+d^2y_{C1}^0d^2y_{C1}^1\dot{x}_{C1}^1)-}{\dot{\phi}\sin(\phi)d^2y_{C1}^0+\cos(\phi)d^3y_{C1}^0\dot{x}_{C1}^0} \tag{64}$$

$$\dot{d}_3 = \frac{\dot{\phi}\cos(\phi)(dy_{C1}^1-dy_{C1}^0)+\sin(\phi)(d^2y_{C1}^1\dot{x}_{C1}^1-d^2y_{C1}^0\dot{x}_{C1}^0)}{+\dot{\phi}\sin(\phi)(1+dy_{C1}^0dy_{C1}^1)-\cos(\phi)(d^2y_{C1}^0dy_{C1}^1\dot{x}_{C1}^0+dy_{C1}^0d^2y_{C1}^1\dot{x}_{C1}^1} \tag{65}$$

$$\dot{d}_4 = \frac{\dot{\phi}\sin(\phi)+\dot{\phi}\cos(\phi)dy_{C1}^1+\sin(\phi)d^2y_{C1}^1\dot{x}_{C1}^1}{d_1}-\frac{d_4}{d_1}\dot{d}_1 \tag{66}$$

$$\dot{d}_5 = \frac{-\dot{\phi}\cos(\phi)+\dot{\phi}\sin(\phi)dy_{C1}^1-\cos(\phi)d^2y_{C1}^1\dot{x}_{C1}^1}{d_1}-\frac{d_5}{d_1}\dot{d}_1 \tag{67}$$

In accordance with the MADYMO 5.1 programmers manual (1994), the kinematical equations of the user joint must be introduced in a subroutine USRJ13. The arguments of this subroutine are:

$$SD = \begin{bmatrix} x_{C1}^0-\cos(\phi)x_{C1}^1+\sin(\phi)y_{C1}^1 \\ y_{C1}^0-\sin(\phi)x_{C1}^1-\cos(\phi)y_{C1}^1 \\ 0 \end{bmatrix} \;,\; SDT = \begin{bmatrix} F \\ \hline 0 \end{bmatrix}\begin{bmatrix} \dot{x}_{C1}^0 \\ \dot{\phi} \end{bmatrix} \;,\; SDTT = \begin{bmatrix} \dot{F} \\ \hline 0 \end{bmatrix}\begin{bmatrix} \dot{x}_{C1}^0 \\ \dot{\phi} \end{bmatrix} \;,\; SDQ = \begin{bmatrix} F \\ \hline 0 \end{bmatrix}$$

$$CD = \begin{bmatrix} \cos(\phi) & -\sin(\phi) & 0 \\ \sin(\phi) & \cos(\phi) & 0 \\ 0 & 0 & 1 \end{bmatrix} \;,\; CDT = \begin{bmatrix} 0 \\ 0 \\ \dot{\phi} \end{bmatrix} \;,\; CDTT = \begin{bmatrix} 0 \\ 0 \\ 0 \end{bmatrix} \;,\; CDQ = \begin{bmatrix} 0 & 0 \\ 0 & 0 \\ 0 & 1 \end{bmatrix}$$

The dimensions are: Q(2x1), QT(2x1), SD(3x1), SDT(3x1), SDTT(3x1), SDQ(3,2), CD(3x3), CDT(3x1), CDTT(3x1), CDQ(3x2). The values for the independent coordinates Q(1), Q(2) and their time derivatives QT(1) and QT(2) at the starting time point of the simulation are defined in the JOINT DOF section of the INITIAL CONDITIONS in the input data file DATA. These values are known to the subroutine USRJ13 as the independent coordinates. A NAG-FORTRAN subroutine C05NBF is used to determine the values of the dependent coordinates by solving the constraint equations (Broekmeulen, 1994). The values of the independent and dependent coordinates can then be used to define the remaining matrices SD, SDT, SDTT, SDQ, CD, CDT, and CDQ. The matrix CDTT is however not specifically defined in the USRJ13 file. The subroutines USRJ13 and USRSY3 can then be compiled and linked with the source code of MADYMO 5.1 and the NAG-FORTRAN libraries to create a new executable.

4.3 The Moeinzadeh 2-Dimensional Knee Model

4.3.1 Introduction

A more comprehensive problem of a 2-dimensional model of the human knee as described by Moeinzadeh et al. (1983) will be simulated in MADYMO to verify the implementation of the joint model. The 2-dimensional model of the articulating joint consists of a moving body segment (the tibia) which is allowed to roll and glide along the surface of a fixed body segment (femur) within the constraints of maintaining point contact and surface normal alignment. The initial configuration is chosen such that the flexion of the tibia with respect to the femur results in a zero strain condition for the ligaments. Figure 4.2 shows the initial configuration of the articulating joint.

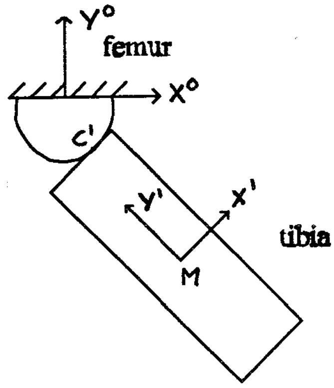

Figure 4.2: The 2-dimensional model of the human knee

The shape of the surface of the body segments is described by polynomials relative to their body fixed coordinate systems (x^0,y^0) and (x^1,y^1) in their respective centers of mass (Figure 4.2). In comparison to the initial problem (Moeinzadeh et al., 1983), the surface polynomial of the femur has changed due to the different orientation of the femur coordinate system:

$$y^0_{C1} = -a_0+a_1x^0_{C1}-a_2(x^0_{C1})^2+a_3(x^0_{C1})^3-a_4(x^0_{C1})^4 \tag{68}$$

The surface of the tibia is described by:

$$y^1_{C1} = b_0+b_1x^1_{C1}+b_2(x^1_{C1})^2 \tag{69}$$

Table 4.1 gives the surface polynomial constants as used by Moeinzadeh and Figure 4.3 shows the shape of the surface profile of the femur.

Table 4.1: Surface polynomial constants of the fixed and moving body segments

femur	tibia
a_0=0.04014	b_0=0.213373
a_1=-0.247621	b_1=-0.0456051
a_2=-6.889185	b_2=1.073446
a_3=-270.4456	
a_4=-8589.942	

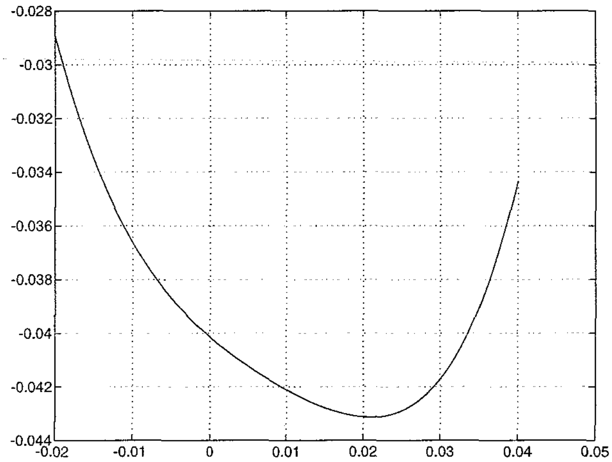

Figure 4.3: Shape of the femoral profile

The mass of the tibia is 3.15 kg and the inertia is 0.05 kgm^2. The initial conditions of the femur-tibia configuration can be derived by solving the constraint equations in the initial configuration. Table 4.2 gives the inital conditions of the configuration.

Table 4.2: Initial values of the independent and dependent variables

x_M^0 [m]	y_M^0 [m]	x_{C1}^0 [m]	y_{C1}^0 [m]	x_{C1}^1 [m]	y_{C1}^1 [m]	ϕ [rad]
0.216	-0.1749	0.042	-0.031695	0.025	0.2129	0.95627

The femur and the tibia are connected by 2 cruciate and 2 collateral ligaments. Table 4.3 provides all the relevant data concerning the ligaments. It should be noted that the initial configuration is such that no initial strains are present in the ligaments. The insertion points of the ligaments are defined relative to the body local coordinate systems in the center of mass of the respective body segments. The constitutive equation of the force as a function of the ligament length only allows a tensile force and is defined as:

$$F_j = K_j*(L_j-L_{0j})^2 \text{ if } L_j \geq L_{0j} \quad , \quad F_j = 0 \text{ if } L_j < L_{0j} \tag{70}$$

in which K_j is the stiffness coefficient, L_j is the current length and L_{0j} is the initial length.

Table 4.3: Values of the stiffnesses, insertions and origins of the ligaments

ligament	x_j^0 [m]	y_j^0 [m]	x_{j1}^1 [m]	y_j^1 [m]	L_{0j} [m]	stiffness K_j [N/m^2]
lateral collateral	0.023	-0.014	0.008	0.163	0.079	$15*10^6$
medial collateral	0.025	-0.019	0.025	0.178	0.056	$15*10^6$
posterior cruciate	0.023	-0.019	-0.005	0.213	0.038	$30*10^6$
anterior cruciate	0.032	-0.024	0.025	0.208	0.018	$35*10^6$

4.3.2 Simulation Results

A numerical model was implemented according to the data provided by Moeinzadeh et al. (1983) and simulations were performed for various applied external forces. Several forces act on the system of the 2 bodies:

- a gravitational force acts on both bodies in the negative y^0-direction.

- an external force F_e which acts in the direction perpendicular to the y^1-axis of the tibia and passes through the center of mass. F_e is defined as a rectangular pulse of duration t_0 and an amplitude A:

$$F_e(t) = A[H(t)-H(t-t_0)] \tag{71}$$

The Moeinzadeh model (Moeinzadeh et al., 1983) shows good with agreement quasi-static experimental investigations reported in the literature. However, it is important to note that the dynamic model is an idealized representation of a very complex anatomical structure. Disagreements with static experimental studies are caused by this approximation and also due to approximate locations of the attachment sites of the ligaments and the 2-dimensional nature of the model in general. For illustrative purposes up to 6° of hyperextension was allowed. Generally a hyperextension of 1-3° is anatomically tolerable beyond which joint failure becomes unavoidable. This can be determined from Figure 4.5.a in which a hyperextension of 6° results in a strain larger than 25% of the posterior cruciate ligament. This would result in a rupture of the ligaments equivalent to an AIS code 3 (Yang et al., 1993).

Figures 4.4-4.5 show the various simulation results of externally applied forces. The shape of Figure 4.4 corresponds to the results obtained by Moeinzadeh et al. (1983) but the peak values are about 10% higher. The initial peaks for the posterior cruciate ligament may be caused by an initial (numerical) pretension of the Kelvin element. In Figure 4.5 it can be seen that due to a faster extension, the peak values occur much earlier in time. The instabilities of the lateral collateral curves can also be seen in Figure 4.4. The curves as shown by Moeinzadeh do not have these instabilities due to the spline through only a few measurement points. It can be seen from Figure 4.6 that the shorter the pulse duration, the sooner the tibia reaches its turning point and the direction of motion changes from flexion to extension.

Results indicate that when the knee is extended (decreasing positive flexion of the tibia), lateral collateral, medial collateral and posterior cruciate ligaments are elongated while the anterior cruciate ligament is shortened. The major role of the collateral ligaments is to ensure varus-valgus and partial internal-external rotation stability. However, the ligaments show very little resistance in the flexion-extension motion of the knee joint.

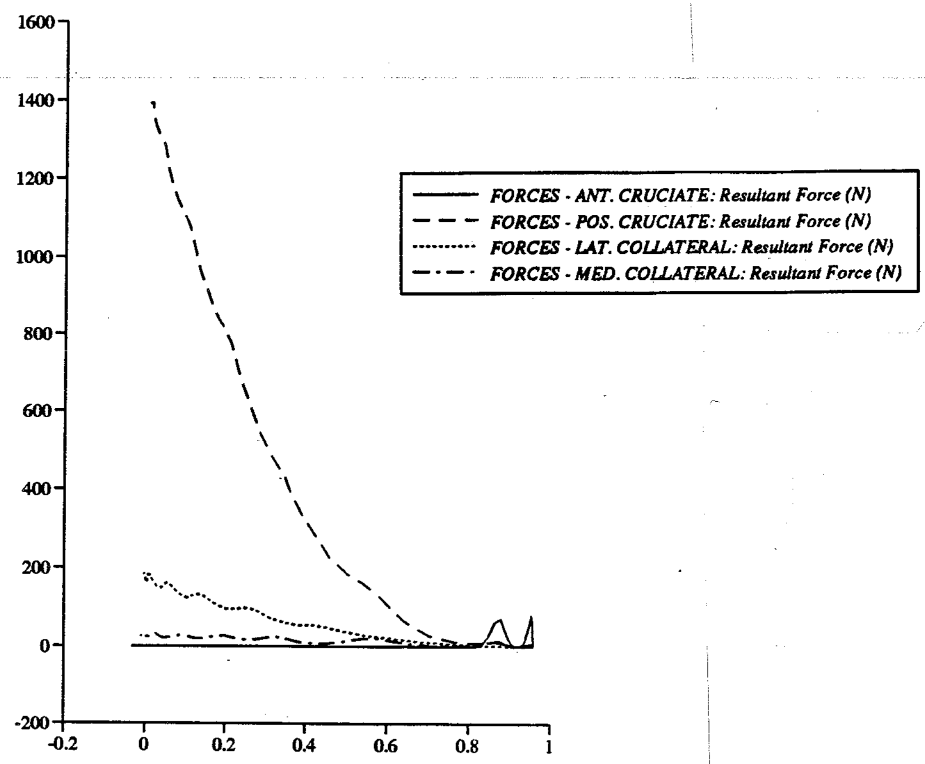

Figure 4.4: Ligament forces as a function of the flexion angle [rad] for an amplitude of 60 N and a pulse duration of 0.05 s.

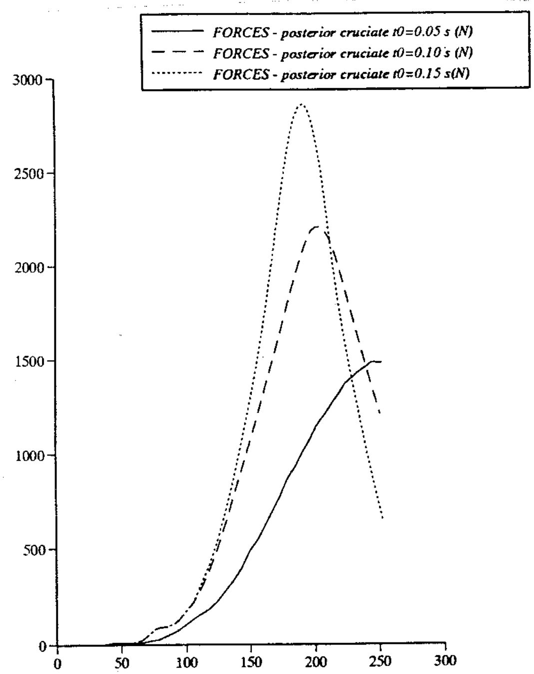

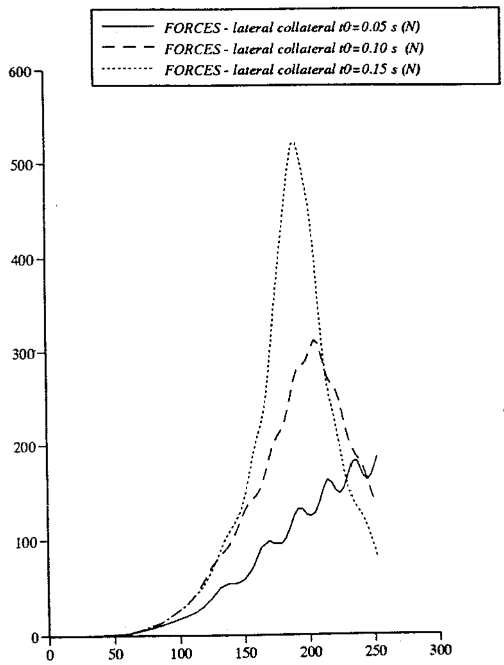

Figure 4.5: (a) Posterior cruciate and (b) lateral collateral ligament forces as a function of time for an amplitude of 60 N and pulse durations of 0.05 s, 0.1 s and 0.15 s.

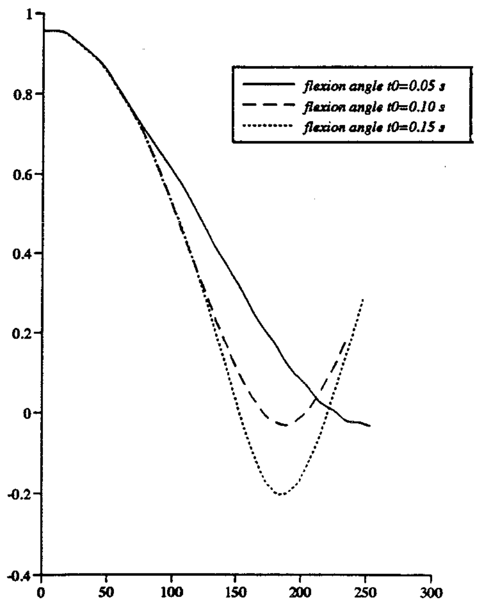

Figure D.6: Flexion angle [rad] as function of time for an amplitude of 60 N and pulse durations of 0.05 s, 0.1 s and 0.15 s.

4.4 Conclusions

The aim of this Chapter was to verify the modelling technique as proposed by Wismans and extended by Moeinzadeh. For this purpose, a 2-dimensional user-joint was implemented in the finite element/multibody code MADYMO 5.1. A verification example (not discussed here) of a rolling disc on a surface, subject to an out of plane external force yielded results which were conform analytic calculations. A more comprehensive problem of a femur-tibia configuration subject to an external force and ligament forces was also simulated. From the simulation results it can be concluded that the implemented dynamic joint model in MADYMO performs according to the required specifications and the results correspond well with results in the literature.

5. Improvements of the Modelling Technique

The modelling technique of Moeinzadeh has in the literature mainly been applied to the description of the articulating motion of the human knee. In this chapter, some possible improvements and extensions of the modelling technique in application to the human knee will be discussed:

- deformability of the bodies has thus far not taken into account but could be implemented in the current model to enable accurate description of the human knee in which a cartilage layer on the femur and tibia allows surface deformation (Blankevoort, 1991). The assumption of point contact should then be replaced with surface contact.

- muscular activity: the muscles stabilize the joint and can generate motion. The possibility to encorporate muscular activity to enable the simulation of gait or active motion has been briefly discussed in section 2.7 but has in literature not been applied to the proposed modelling technique.

- introduction of damping: in the configuration of the human knee for example the surfaces of the femur and tibia are covered by articular cartilage which has viscoelastic properties. These visco-elastic properties have a significant influence on the motion characteristics during dynamic tests.

- the modelling technique can be enhanced to encorporate friction if for example the synovial fluid in the human knee does not have the required tribological properties and friction does play a role in the articulating motion.

- the description has to be extended if more than two bodies participate in the arcticulating joint, in the human knee for example the pattela-femur contact (Tümer et al., 1993) is usually modelled as an external force (Wismans, 1980) but can then be directly implemented in the model.

- the numerical solution procedure needs to be optimized as there is as yet no agreement concerning the most efficient solution procedure. The present methods proposed by Engin and Abdel-Rahman offer no reliable reason for comparison as specific information such as difficulty and computational effort is not given. Explicit integration is a possible method to be adopted to solve the differential equations. A more efficient method to obtain a solution to the equations is achieved by using algorithms in the NAG FORTRAN library.

References

- Abdel-Rahman, E., Hefzy, M.S., A Two-Dimensional Dynamic Anatomical Model of the Human Knee Joint, Journal of Biomechanical Engineering, Vol. 115, pp. 357-365, 1993.

- Blankevoort, L., Passive Motion Characteristics of the Human Knee Joint (Experiments and Computer Simulations), PhD. Thesis, Katholieke Universiteit Nijmegen, Nijmegen, 1991.

- Broekmeulen, M.C.C., The Dynamical Motion of a 2-Dimensional Knee Model: Implementation in Fortran 77 (in Dutch), WFW Report No. 94.148, Eindhoven University of Technology, Eindhoven, 1994).

- Engin, A.E., Moeinzadeh, M.H., Dynamic Modelling of Human Articulating Joints, Mathematical Modelling, Vol. 4, pp. 117-141, 1983.

- Engin, A.E., Berme, N., Akkas, N., Dynamic Modeling of Human Articulating Joints, Biomechanics of Normal and Pathological Human Articulating Joints, pp. 189-213, Martinus Nijhoff Publishers, Dordrecht, 1985.

- Engin, A.E., Tümer, S.T., An Innovative Approach to the Solution of Highly Nonlinear Dynamics Problems Associated with Joint Biomechanics, ASME Biomechanics Symposium, AMD-Vol. 120, pp. 225-228, 1991.

- Engin, A.E., Tümer, S.T., On the Applicability of the Classical Impact Theory to the Dynamics of Human Joints, Engineering Systems Design and Analysis, PD-Vol. 47-2, pp. 67-73, 1992.

- Engin, A.E., Tümer, S.T., Improved Dynamic Model of the Human Knee Joint and Its Response to Impact Loading on the Lower Leg, Journal of Biomechanical Engineering, Vol. 115, pp. 137-143, 1993.

- Grood, E.S., Suntay, W.J., A Joint Coordinate System for the Clinical Description of Three-Dimensional Motions: Application to the Knee, Journal of Biomechanical Engineering, Vol. 105, pp. 136-144, 1983.

- Hefzy, M.S., Grood, E.S., Review of Knee Models, Appl. Mech. Rev. Vol. 41, no 1, pp. 1-13, 1988.

- Karlsson, J.O.M., Murphy, M.C., Mann, R.W., Using Axiodes to Represent Biokinematic Data, Proceedings of the International Symposium on 3-D Analysis of Human Movement, July 28-31, Montreal, Canada, pp. 57-58, 1991.

- MADYMO Users Manual, Version 5.1, TNO Road Vehicles Research Institute, Delft, 1994.

- Moeinzadeh, M.S., Two and Three-dimensional Dynamic Modeling of Human Joint Structures with Special Applications to the Knee Joint, PhD. Thesis, Ohio State University, Ohio, 1981.

- Moeinzadeh, M.H., Engin, A.E., Akkas, N., Two-Dimensional Modelling of Human Knee Joint, Journal of Biomechanics, Vol. 16, No. 4, pp. 253-264, 1983.

- Moeinzadeh, M.H., Engin, A.E., Response of a Two-Dimensional Dynamic Model of the Human Knee to the Externally Applied Forces and Moments, Journal of Biomedical Engineering, Vol. 5, No. 4, pp. 281-291, 1983.

- Moeinzadeh, M.H., Engin, A.E., Dynamic Modeling of the Human Knee Joint, Computational Methods in Bioengineering, Winter Annual Meeting of the ASME, Chicago, 1988.

- Shabana, A.A., Dynamics of Multibody Systems, John Wiley & Sons, New York, 1989.

- Thunnissen, J.G.M., Muscle Force Prediction During Human Gait, PhD. Thesis, Twente University of Technology, Enschede, 1993.

- Tümer, S.T., Engin, A.E., Three-Body Segment Dynamic Model of the Human Knee, Journal of Biomechanical Engineering, Vol. 115, pp. 350-356, 1993.

- Wismans, J.S.H.M., A Three-Dimensional Mathematical Model of the Human Knee Joint, PhD. Thesis, Eindhoven University of Technology, Eindhoven, 1980.

- Woltring, H.J., 3-D Attitude Representation: a New Standardization Proposal, Biomechanics Seminar, Vol. 4, pp. 58-61, 1990.

- Wongchaisuwat, C., Hemami, H., Buchner, H.J., Control of Sliding and Rolling at Natural Joints, Journal of Biomechanical Engineering, Vol. 106, pp. 368-375, 1984.